Beyond bond links in complex networks:Local bridges, global bridges and silk links

Chung-Yuan Huang [a], Wei-Chien-Benny Chin [b,*], Yu-Hsiang Fu [c], Yu-Shiuan Tsai [d]

[a] Department of Computer Science and Information Engineering, School of Electrical and Computer Engineering, College of Engineering, Chang Gung University, 259 Wen Hwa 1st Road, Taoyuan 333, Taiwan
[b] Department of Geography, National Taiwan University, 1 Sec. 4, Roosevelt Road, Taipei 10617, Taiwan
[c] Department of Computer Science, National Chiao Tung University, 1001 Ta Hsueh Road, Hsinchu 300, Taiwan
[d] Department of Computer Science and Engineering, National Taiwan Ocean University, 2 Pei-Ning Road, Keelung 20224, Taiwan

H I G H L I G H T S

- An identification algorithm for determining hierarchical link types is described.
- Multi-hierarchy level link types are identified using the common neighbor concept.
- Two applications are demonstrated: fingerprint analysis and network partitioning.
- Fingerprint analysis is used to compare topological structures among networks.
- Hierarchical link structures are used to partition networks into communities.

A R T I C L E   I N F O

A B S T R A C T

Many network researchers use intuitive or basic definitions when discussing the importance of strong and weak links and their roles. Others use an approach best described as "if not strong, then weak" to determine the strengths and weaknesses of individual links, thus deemphasizing hierarchical network structures that allow links to express different strength levels. Here we describe our proposal for a hierarchical edge type analysis (HETA) algorithm for determining link types at multiple network hierarchy levels based on the common neighbor concept plus statistical factors such as bond links, kth-layer local bridges, global bridges, and silk links—all generated during long-term network development and evolution processes. Two sets of networks were used to validate our proposed algorithm, one consisting of 16 networks employed in multiple past studies, and one consisting of two types of one-dimensional small-world networks expressing different random rewiring or shortcut addition probabilities. Two applications with potential for developmental contributions are demonstrated: a network fingerprint analysis framework, and a hierarchical network community partition method.

1. Introduction

Networks consist of large numbers of nodes and links, with each link indicating a specific type of interactive effect between two adjacent nodes—for example, predator–prey relations in food chains, friendships in acquaintance

* Corresponding author.
E-mail addresses: gscott@mail.cgu.edu.tw (C.-Y. Huang), wcchin.88@gmail.com (W.-C.-B. Chin).

networks, and input–output relationships in electronic circuits. Following an abstraction process, many complex systems can be represented as networks, and researchers now use static topology analyses, dynamic process simulations, and other approaches to explore the nonlinear dynamic, emergent, and macro-level results of entire networks according to micro-level interactions involving network elements [1].

Regarding link properties, Granovetter [2] used his famous job search experiment to show how weak links in acquaintance networks serve not only as important pipelines for transmitting information or transferring objects to groups with longer paths, but also as conduits for disseminating useful information to network members. Weak links are conducive to improving network stability [3]; McCann et al. [4] note that when network nodes representing species, individuals, or computers are at risk of attack, surviving sub-networks can continue operations so as to prevent crashes or collapses, as long as a weak-link majority is retained. In contrast, despite the weaknesses of strong links in transferring information in order to maximize network diffusion coverage, they still have the potential to strengthen, save messages, transfer complex messages, and support close relationships among group members [5,6]. Thus, group members with strong links are less likely to disappear from networks.

Using a combination of strong and weak link concepts and knowledge complexity to study the impacts of different link properties, Hansen [7] found that both strong and weak links are capable of transferring knowledge and information, although each has its own pros and cons. For example, weak links are likely to hinder knowledge transfer while concurrently improving knowledge search efficiency, regardless of knowledge complexity. In contrast, strong links do not contribute directly to knowledge searches, but in situations involving high levels of knowledge complexity they are more likely to become powerful factors in knowledge transfers between institutional and other sectors. Hansen concluded that in terms of organizational units, coexistence is essential due to the importance of both types of links.

Putnam's [8] description of bridge and bond links associated with social capital indicates some similarities with a strong/weak tie concept in which the bridge form consists of outreach-type links between members of external or other heterogeneous groups—links that support the attainment of new information and opportunities. He describes the bond type as cohesive links connecting members of internal or other homogeneous groups, thus facilitating support and encouragement. Accordingly, in business environments or networks, the greater the number of social capital bond types that employees have, the greater their opportunities for better positions with higher salaries. This tie strength concept is still being used in analyses of social interactions and economic development (see, for example, [5,9–13].

Regarding link properties, many social network researchers have adopted non-exhaustive definitions of links based on intuition and relied on oversimplified definitions involving strong–weak dichotomies. However, networks have hierarchical structures, and links at different network levels are likely to exhibit a range of strong/weak properties and influences—an idea that conflicts with previous assertions of links having single, unchanging strength properties [14–16]. Network researchers who have utilized domain knowledge to quantify the strong/weak properties of network links include Barrat et al. [17], Onnela et al. [18], and Papakyriazis and Boudourides [19]. There is evidence indicating that sexual and ecological networks have different parameters for quantifying strong/weak link properties: in sexual networks, quantification involves measuring sexual intercourse frequencies involving pairs of individuals during a fixed time period, while in ecological networks, certain inter-species links indicate predator–prey relationships quantified as numbers or ratios of prey caught by predators during a fixed time interval.

For all network types, the core problem of using domain knowledge to quantify network properties is associated with the dual difficulties of collecting quantitative data and determining their accuracy. Accordingly, straightforward efforts to quantify the strengths or weaknesses of individual links at multiple hierarchy levels often entail the use of topological properties derived from network development and/or evolution over time, a process that comes at the expense of considering the domain knowledge of a network. Today's researchers are acutely aware that the topological properties and hierarchical structures of networks are not generated "randomly and occasionally", but according to certain principles such as "artificial design" or "natural evolution". In this paper we will address the properties and roles of network links from a topological perspective.

Evaluating link strength is essential for understanding network topological structures [20,21]. Determining link hierarchies according to strong/weak relationships can assist in the identification of boundaries within networks and provide insights to the hierarchical structures of communities [15,22,23]. In addition, link hierarchy knowledge also provides useful information regarding network-related issues such as influential spreaders and network diffusion [24], link and network development [25], and network structure redundancy [26].

As part of our effort to comprehensively capture the strong/weak link concept, we propose using hierarchy-based definitions of network bond links and bridges instead of existing definitions that we believe are overly simplistic, non-exhaustive, and excessively reliant on intuition. Since they represent the strengths of connections between pairs of groups in a network, bridges exert significant influence on long-distance message transmission [18,21,27]. In their role of representing the strength of connections between two individuals within a group, bond links exert strong influences on resource sharing [28–30]. Given that the effects of bridge and bond links vary greatly due to their different network roles, we developed a hierarchical edge type analysis (HETA) algorithm for determining four link types – bond links, kth-layer local bridges, global bridges and silk links – at multiple network hierarchy levels, based on the common neighbor concept

and statistical factors, and generated during long-term network development and evolution.

In this paper we will describe and demonstrate two applications with potential for developmental contributions: a network fingerprint analysis framework, and a hierarchical network community partition method. Since the four hierarchical network link types can be integrated in a manner that reflects a network's topological structure, we will use their percentages as fingerprints for characterizing networks. We believe these kinds of network data can be used for comparison purposes in future studies, especially in cases where links in networks (either new or previously analyzed) have similar percentages.

2. Identification algorithm and related methods

Ever since Granovetter [2] first proposed the strong/weak tie idea, network link strength has been the focus of a large number of social and complex network analyses, and over time the literature has expanded to include many detailed discussions of bond links and bridges. Researchers have noted that when the number of common friends connected to nodes on both sides of links decreases, the potential increases for them to take on the forms of different groups connected by links that serve as message bridges. Further, as the number of common friends consisting of nodes on both sides of links grows, they increasingly take on the appearance of a single group with close internal bond links. Bridges in networks transmit messages between groups (including those separated by long distances), while bond links tend to retain messages, thus making it unlikely for them to disappear. The two types of links have different replaceability properties. The loss of a bridge increases the likelihood of messages not being delivered to their intended destinations, or of much longer transmission times. Bond links are more easily replaced than bridges—when a bond link disappears, messages can still be transmitted quickly via alternative short paths.

Here we will describe an algorithm based on the common neighbor concept for identifying four complex network link types: silk, bond, multi-layer local bridge, and global bridge. According to Bollobás's [31] original bridge definition in a network context, the removal of any bridge splits one network into two sub-networks. Here we extend the bridge definition to include multi-layer local and global bridges.

Conceptually speaking, a global bridge is a link that, if removed, creates one of two situations: (a) a network split into two sub-networks, or (b) a need for two endpoints to connect via an alternative path whose length is at a minimum equal to the network's average shortest path length [32]. Silk links represent a special global bridge type in that their removal results in isolated endpoints. While unique, silk links are not as critical as other kinds of global bridges for the topological structure of a network. In contrast, bond links connect pairs of nodes sharing a large number of common friends, therefore their removal does not cause serious damage to a network's topological structure. Global bridge and bond links are considered two extremes in terms of replaceability, with multi-layer local bridge links somewhere in-between—the higher the local bridge layer, the lower the replaceability value. A working definition and procedures for identifying the four link types are presented in the Algorithm 1 pseudo-code. The three-step flowchart in Fig. 1 illustrates our goal to use topological replaceability to identify hierarchical link types.

The three-step flowchart shown in Fig. 1 illustrates our goal of determining hierarchical link types according to topological replaceability. Our proposed identification algorithm was implemented as a Python 2.7 program code using NetworkX and Matplotlib packages to take advantage of their code readability and package support characteristics, while accepting the disadvantage of slower execution times compared to compiled programming language (e.g. C and C++). Our Python program code can be extended to support new applications and run on most operating systems, including Linux, MacOS and Windows. The input data used for testing and validating this algorithm and related applications are from two sets of networks, one consisting of 16 well-known networks previously employed in multiple studies (Table 1), the other consisting of two types of one-dimensional small-world networks expressed according to different random rewiring and shortcut addition probabilities. All Python program output data were processed using Microsoft Excel. Readers interested in source code and input network data for specific research requirements are encouraged to contact the corresponding author or use GitHub for direct downloads (https://github.com/canslab1/Identification-Algorithm/).

Algorithm 1 Identification Algorithm for Determining Hierarchical Link Types

Input: network $G = (V, E)$, where V is the node set and E the link set
Output: 3-dimensional matrix, *Type*, which denotes the hierarchical types of all links at all network layers

comment Step #1: Calculate common neighbor ratios for all links at all layers of network G
$K_{max} \leftarrow$ one-half the average shortest path length of network G (Ref. to Eqs. 3-4)
for each link (u, v) **in** link set E of network G **do loop**
    for each layer k **from** 1 **to** K_{max} **do loop**
        Calculate the kth-layer common neighbor ratio $R_{u,v}^k$ for the link (u, v) of network G (Ref. to Eqs. 1-2)
    end for
end for /* Both time and space complexities are $O(|E| \times Radius)$ in Step #1. */

comment Step #2: Generate set of randomized networks for comparisoning with network G
Generate 1000 randomized networks (i.e., $RG = \{G_1^R, G_2^R, ..., G_{1000}^R\}$ where RG is a set composed of 1000 randomized
        networks and G_i^R the ith randomized network) corresponding to network G using a switching
        randomization algorithm
for each layer k **from** 1 **to** K_{max} **do loop**
    for each randomized network G_i^R **in** RG **do loop**
        for each link (u, v) **in** link set E_i^R of randomized network G_i^R **do loop**
            Calculate the kth-layer common neighbor ratio $R_{u,v}^k$ for link (u, v) in randomized network G_i^R
        end for
    end for
    comment Calculate the kth-layer's external threshold T_E^k for Step #3.2
$$Mean_E^k \leftarrow \frac{\sum_{i=1}^{|RG|} \sum_{(u,v) \in E_i^R} R_{u,v}^k}{|RG| \times |E|}; \quad SD_E^k \leftarrow \sqrt{\frac{\sum_{i=1}^{|RG|} \sum_{(u,v) \in E_i^R} (R_{u,v}^k - Mean_E^k)^2}{|RG| \times |E|}}; \quad T_E^k \leftarrow Mean_E^k + 2SD_E^k$$
end for /* Both time and space complexities is $O(|RG| \times |E| \times Radius)$ in Step #2 */

comment Step #3.1: Identify silk links of network G
for each link (u, v) **in** link set E of network G **do loop**
    if the degree of node u is equal to 1 **or** the degree of node v is equal to 1 **then**
        $Type_{u,v}^0 \leftarrow$ **SILK** /* at layer 0 */
        $Pass_{u,v} \leftarrow$ **FALSE**
    else
        $Pass_{u,v} \leftarrow$ **TRUE**
    end if
end for /* Both time and space complexities are $O(|E|)$ in Step #3.1 */

comment Step #3.2: Identify bond links and local bridges at all network layers
for each layer k **from** 1 **to** K_{max} **do loop**
    $Candidate\_Bridges^k \leftarrow$ empty set {}
    for each link (u, v) **in** link set E of network G **do loop**
        if $Pass_{u,v}$ is **FALSE then**
            comment copy link type from the $(k-1)$th-layer to kth-layer
            $Type_{u,v}^k \leftarrow Type_{u,v}^{k-1}$
        comment Step #3.2.1 Whether the link sereves as a bond link
        else if $R_{u,v}^k$ is greater than or equal to T_E^k **then**
            $Type_{u,v}^k \leftarrow$ **BOND LINK**
            $Pass_{u,v} \leftarrow$ **FALSE**
        else
            $Candidate\_Bridges^k \leftarrow Candidate\_Bridges^k \cup R_{u,v}^k$
        end if
    end for
    if $Candidate\_Bridges^k$ is not an empty set {} **then**
        comment Step #3.2.2 Calculate the kth-layer's internal threshold T_I^k for the kth-layer local bridges
        $T_I^k \leftarrow Mean(Candidate\_Bridges^k) - SD(Candidate\_Bridges^k)$
        for each link (u, v) **in** link set E of network G **do loop**
            if $Pass_{u,v}$ is **TRUE** and $R_{u,v}^k$ is greater than T_I^k **then**
                $Type_{u,v}^k \leftarrow$ **kTH LAYER LOCAL BRIDGE**
                $Pass_{u,v} =$ **FALSE**
            end if
        end for
    end if
end for /* Both time and space complexities are $O(|E| \times Radius)$ in Step #3.2 */

comment Step #3.3: Identify network G global bridges
for each link (u, v) **in** link set E of network G **do loop**
    if $Pass_{u,v}$ is **TRUE then**
        $Type_{u,v}^{Radius} \leftarrow$ **GLOBAL BRIDGE**
    end if
end for /* Time and space complexities are $O(|E|)$ and $O(|E| \times Radius)$ respectively in Step #3.3 */

return *Type*

Note: Overall time and space complexities are $O(|RG| \times |E| \times Radius)$

The common neighbor concept can be used to identify link characteristics at multiple network levels, with "first-layer common neighbor" defined as the degree to which nodes at both ends of a link are acquainted with each other's friends. An undirected, non-weighted network G without self-loop or parallel edges can be expressed as (V, E), where V is a set

Table 1
Network datasets organized by discipline.

Discipline	Network code	Number of nodes	Number of links	Network density	Average shortest path length	Average clustering coefficient	Source
Social Sciences	rdgam	12	28	0.4242	2.0909	0.8306	[33,34]
	women	16	50	0.4167	1.8167	0.8182	[35]
	football	115	613	0.0935	2.5082	0.4032	[22,36]
	jazz	198	2742	0.1406	2.235	0.6175	[37]
	lesmis	77	254	0.0868	2.6411	0.5731	[38]
	camp92	18	35	0.2288	2.6601	0.5685	[39]
	prisonInter	67	142	0.0642	3.3546	0.3099	[40,41]
	karate	34	78	0.1390	2.4082	0.5706	[42]
	leader	32	80	0.1613	2.2964	0.3266	[40,43]
	ragusa16	24	68	0.2464	2.0942	0.3427	[44]
	dolphins	62	159	0.0841	3.357	0.2590	[45]
	florentine	15	20	0.1905	2.4857	0.1600	[46]
Biology	celegans	297	2148	0.0489	2.4553	0.2924	[32,47]
Electronics	s208	122	189	0.0256	4.9278	0.0591	[48,49]
Network theory	ba_sfn	100	196	0.0396	3.0313	0.1343	[50]
	k-core	26	31	0.0954	3.4708	0.1607	[51]

of n nodes resulting in $V = \{v_1, v_2, v_3, \ldots, v_n\}$ and $n = |V|$, and E is a set of m links resulting in $E = \{e_1, e_2, e_3, \ldots, e_m\}$ and $m = |E|$, with each link expressed as a node pair (v_i, v_j) where $v_i, v_j \in V$ and $1 \leq i \neq j \leq n$. For each link (v_i, v_j) in E, the first-layer neighbors of end node v_i constitute the set of neighbor nodes that excludes node v_j at the other end—in other words, $V_i^{1,j} = \{v_k | (v_i, v_k) \in E\} - \{v_j\}$. Thus, for each link (v_i, v_j) in E, the first-layer common neighbor ratio $R_{i,j}^1$ is expressed as

$$R_{i,j}^1 = \begin{cases} \frac{\left|V_i^{1,j} \cap V_j^{1,i}\right|}{\min\left(\left|V_i^{1,j}\right|, \left|V_j^{1,i}\right|\right)} & \text{if } \left|V_i^{1,j}\right| > 0 \,\&\, \left|V_j^{1,i}\right| > 0 \\ 0 & \text{otherwise} \end{cases} \tag{1}$$

with a range of 0 to 1. Superscript 1 in $R_{i,j}^1$ denotes "first-layer", subscript i,j denotes link (v_i, v_j), and $\min(|V_i^{1,j}|, |V_j^{1,i}|)$ is the smaller of the two first-layer neighbor numbers of nodes v_i and v_j. The number of first-layer common neighbors cannot exceed the number of first-layer neighbors of either individual node. The higher the first-layer common neighbor ratio, the higher the closeness value and the greater the replaceability of the link between them.

Also according to the common neighbor concept, calculations for kth-layer neighbor $V_i^{k,j}$ for any node v_i in V and kth-layer common neighbor ratio $R_{i,j}^k$ for any link (v_i, v_j) in E can be expressed as

$$R_{i,j}^k = \begin{cases} \frac{\left|V_i^{k,j} \cap V_j^{k,i}\right| + \left|V_i^{k-1,j} \cap V_j^{k,i}\right| + \left|V_i^{k,j} \cap V_j^{k-1,i}\right|}{\min\left(\left|V_i^{k,j}\right|, \left|V_j^{k,i}\right|\right) + \min\left(\left|V_i^{k-1,j}\right|, \left|V_j^{k,i}\right|\right) + \min\left(\left|V_i^{k,j}\right|, \left|V_j^{k-1,i}\right|\right)} & \text{if } \left|\left(V_i^{k,j} \cap V_j^{k,i}\right) \cup \left(V_i^{k-1,j} \cap V_j^{k,i}\right) \cup \left(V_i^{k,j} \cap V_j^{k-1,i}\right)\right| > 0 \\ 0 & \text{if } \left|\left(V_i^{k,j} \cap V_j^{k,i}\right) \cup \left(V_i^{k-1,j} \cap V_j^{k,i}\right) \cup \left(V_i^{k,j} \cap V_j^{k-1,i}\right)\right| = 0 \end{cases} \tag{2}$$

$$V_i^{k,j} = \begin{cases} \left\{v_y | \forall v_x \in V_i^{k-1,j} : (v_x, v_y) \in E\right\} - \cup_{p=1}^{k-1} V_i^{p,j} - \{v_i, v_j\} & \text{if } k > 1 \\ \left\{v_y | (v_i, v_y) \in E\right\} - \{v_j\} & \text{if } k = 1 \end{cases} \tag{3}$$

where superscripted k denotes a layer number in a range from 1 to k_{max}, which is one-half the average shortest path length between any two network nodes [32] (Eq. (4)).

Fig. 2 shows a shared neighbor (first and second layers) for a link between A and B. The first-layer neighbor set for node A is $V_A^{1,B} = \{p, u, v, w, s\}$ and second-layer neighbor set $V_A^{2,B} = \{q, t\}$; the first-layer neighbor set for node B is $V_B^{1,A} = \{r, u, v, w, t\}$ and second-layer neighbor set $V_B^{2,A} = \{q, s\}$. Note that nodes u and v are first-layer neighbors of nodes A and B, therefore they are not included in the second-layer neighbor set shown in Eq. (3), despite the presence of a link between u and v. The first-layer common neighbor set contains nodes u, v and w, and the second layer neighbor set consists of $V_A^{2,B} \cap V_B^{2,A} = \{q\}$, $V_A^{1,B} \cap V_B^{2,A} = \{s\}$, and $V_A^{2,B} \cap V_B^{1,A} = \{t\}$. As this example demonstrates, even though the alternative path length between nodes A and B (i.e., A-s-t-B) is 3, an odd number, nodes s and t are only ignored if $V_A^{2,B} \cap V_B^{2,A}$ is considered—in other words, nodes s and t do not match the descriptions of both first- and second-layer neighbors. The common neighbor ratio helps measure the number of common nodes for each layer starting from the two endpoints of any link (A, B). In this example there are two common neighbors in the A-s-t-B path, and one common neighbor in the A-p-q-r-B path; accordingly, second-layer common neighbors consist of three sets of nodes ($V_A^{2,B} \cap V_B^{2,A}$, $V_A^{1,B} \cap V_B^{2,A}$, and $V_A^{2,B} \cap V_B^{1,A}$). The Eq. (2) denominator is the largest possible number of common neighbors shared by the
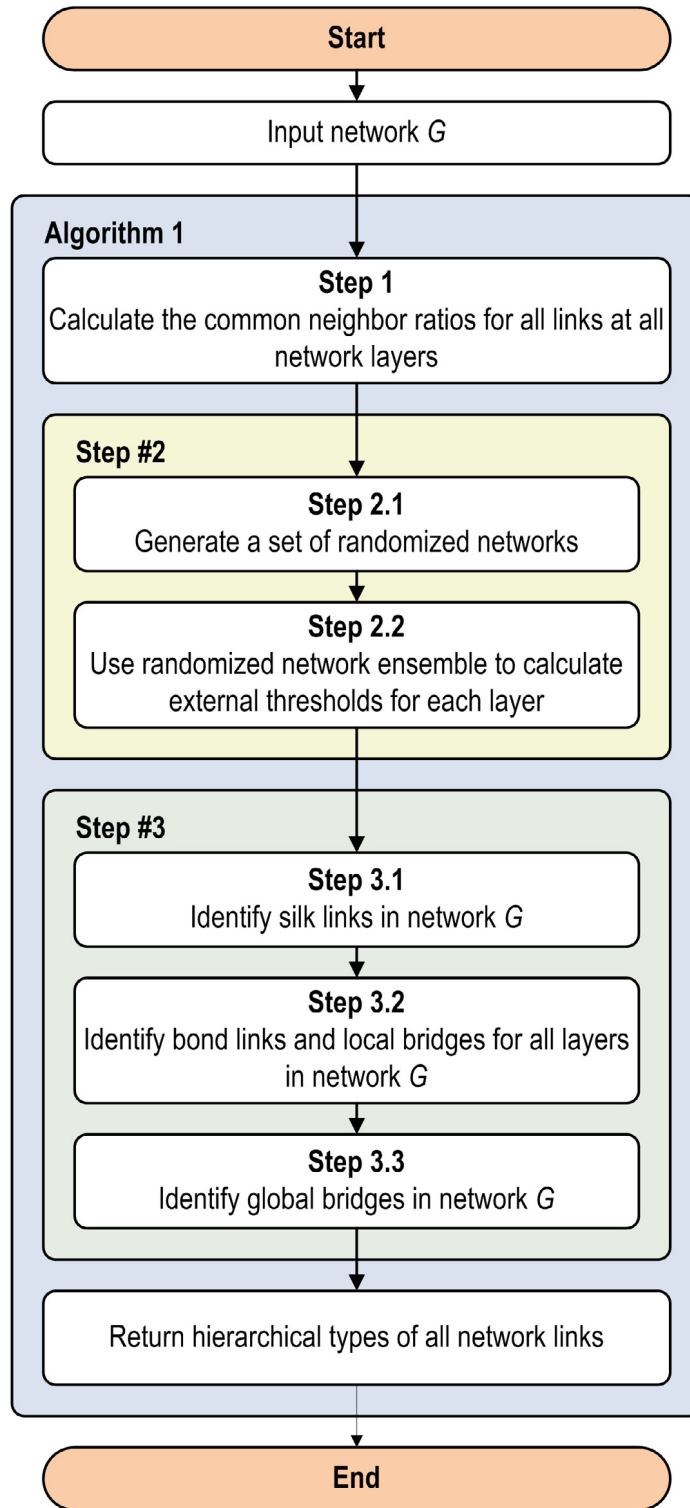
Fig. 1. Three-step flowchart corresponding to the Algorithm 1 pseudo-code.

three second-layer nodes—that is, the smaller of either the number of kth-layer neighbors of nodes A and B or the number of $(k − 1)$th-layer neighbors for the same two nodes.
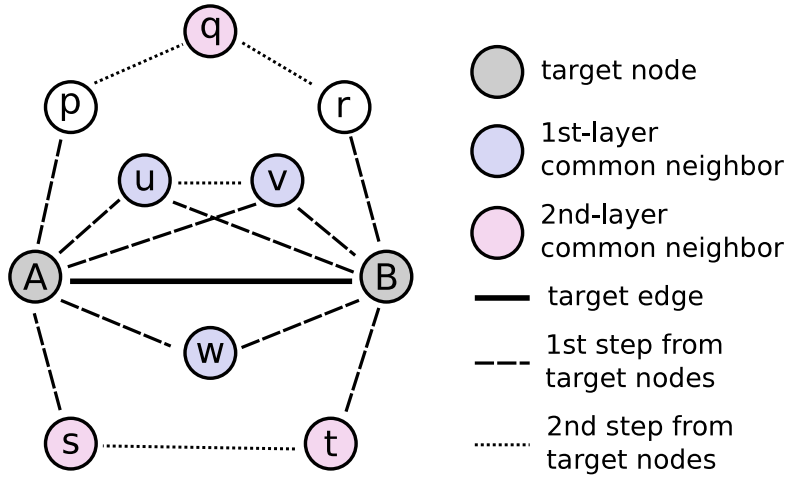
Fig. 2. A sample network for describing the second layer common neighbors for the link between A and B.

The average shortest path length of a network indicates the average number of steps between all possible node pairs in the network [32]. Accordingly, a sparsely connected network will have a longer average shortest path length compared to a densely connected network because the latter has more node-connecting shortcuts, thus reducing the average distance between them. In this study, the k_{max} max-layer was used when searching for common neighbors starting from the nodes at the ends of links, therefore k_{max} was defined as one-half the average shortest path length. k_{max} can be expressed as Eq. (4), with *ShortestPathLength* (u, v) defined as the length of the shortest path between nodes u and v, and with n the total number of nodes. Since average shortest path length in a real-world network typically varies according to the logarithm of n [48,52], $k_{max} \propto \log n$. Individuals in social networks generally need to use resources to maintain ties, therefore m is bound so that large networks remain sparse.

$$k_{max} = \text{floor} \left(\frac{1}{2} \left(\frac{\sum_{u,v \in N \wedge u \neq v} ShortestPathLength\,(u, v)}{(n \times (n - 1))\,/2} \right) \right) \tag{4}$$

At the beginning of Step 2 in Algorithm 1, a set of randomized networks (expressed as $RG = \{G_1^R, G_2^R, \ldots, G_{1000}^R\}$, where RG is a set consisting of 1000 randomized networks and G_i^R the ith randomized network) was used to make comparisons with the network being investigated. Randomized networks were generated from copies of the investigated network (e.g., the initial $G_i^R \leftarrow$ copy of network$G$) using a well-known switching randomization algorithm [40,52–55]. The algorithm repeatedly switches between two randomly chosen pairs of nodes in the copied network at each step until the copied network is randomized to a previously determined target. During each step, two link pairs (e.g., (a, b) and (c, d)) are randomly sampled with replacements from the current set of links, with the sampling process based on a uniform probability distribution. If $a \neq d$, $c \neq b$, and links (a, d) and (c, b) do not yet exist, they are added to the network at the same time that (a, b) and (c, d) are removed. After Q x m steps, where m is the number of links and Q a number suggested by Milo et al. [54] as 100, the copied network is considered randomized. Since node degrees are preserved as part of this switching process, the number of nodes, number of links, and node degree distribution are all conserved in randomized networks corresponding to the investigated network.

After generating an ensemble of randomized networks, we calculated external T_E^k and internal T_I^k thresholds for use in link classification. Detailed descriptions of the calculation procedures are respectively shown in Steps 2 and 3.2 of Algorithm 1. The value of T_E^k is calculated via the external mean of $R_{i,j}^k$ ($Mean_E^k$) and the external standard deviation of $R_{i,j}^k$ (SD_E^k), based on the randomized network (RG); the T_E^k calculation is given as Eq. (5). While the sampling distribution for generating randomized networks is uniform, randomized $R_{i,j}^k$ is likely to have a normal distribution, meaning that a link's $R_{i,j}^k$ value will approximate the external mean—statistically speaking, 95% of $R_{i,j}^k$ should be between $Mean_E^k - 2SD_E^k$ and $Mean_E^k + 2SD_E^k$. Accordingly, we used T_E^k as the upper threshold, indicating that any $R_{i,j}^k$ that exceeds T_E^k has a statistically significant high common neighbor ratio. The kth-layer's external threshold T_E^k is used to determine whether a link passed from the $(k - 1)$th-layer is a bond link at the kth-layer. Whereas T_E^k is calculated based on the randomized network, T_I^k is calculated based on candidate links passed from the preceding $(k - 1)$th-layer to the current kth-layer. Further, T_I^k is calculated based on the internal means ($Mean_I^k$) and internal standard deviations (SD_I^k) of the $R_{i,j}^k$ values of candidate links (expressed as Eq. (6)). In other words, each candidate link's $R_{i,j}^k$ value is compared to the distribution of $R_{i,j}^k$ values for all candidate links. Candidate links with common neighbor ratios greater than T_I^k are identified as kth-layer local bridges, and other candidate links move to the next $(k + 1)$th-layer. In short, only those candidate links with relatively low common

neighbor ratios in the kth-layer remain undefined and consequently move to the next layer. Global bridges are identified according to their highest layer's common neighbor ratio $R_{i,j}^{k_{max}}$, whether they are less than the highest layer's external threshold $T_E^{k_{max}}$, and whether they are less than or equal to the highest layer's internal threshold $T_I^{k_{max}}$.

$$T_E^k = Mean_E^k(RG) + 2SD_E^k(RG) \tag{5}$$

$$T_I^k = Mean_I^k(candidate\ links) - SD_I^k(candidate\ links) \tag{6}$$

When considering all of the steps in Algorithm 1, time and space complexities are identical. Accordingly, $O(m \cdot |RG| \cdot k_{max})$, where m is the number of links, $|RG|$ the number of randomized networks, and k_{max} varies according to the logarithm of the n number of nodes in a real-world network ($k_{max} \propto \log n$) (Eq. (4)).

Fig. 3 shows the calculation framework and the four identified link types. The example network presented in Fig. 3a consists of 13 nodes and 28 links, with a diameter of 5 units and average shortest path length of 2.282 units. Identification procedures for the four link types are shown in Figs. 3b–3e, with the final results displayed in Fig. 3f. Using Fig. 3 as an example, the four link types can be described as follows:

1. Silk links. The removal of a silk link results in the isolation of one of the two end nodes that were originally connected by the link. A link (u, v) is identified as a silk link if and only if the degree of either u or v equals 1. If the link between E and F in Fig. 3b is removed, F becomes isolated, making the link a silk link.

2. Bond links. Since nodes at both ends of a bond link have many friends in common, multiple alternative paths for transmitting messages remain when the link is removed. Starting from the first layer to the k_{max} layer, if the type of link (u, v) is unknown at a lower ($k - 1$)th layer, the link is identified as a bond link if and only if its common neighbor ratio $R_{u,v}^k$ exceeds an external threshold T_E^k. In Fig. 3c, since the T_E^1 external threshold = 0.8506, all blue links with $R_{u,v}^1 = 1$ are bond links.

3. Local bridges. Even though the proportion of common friends between nodes at the two ends is low, they are connected via longer friend chains consisting of friends of friends of friends and so on. Since alternative paths are available when a local bridge is removed, the alternative path of a kth-layer local bridge (if one exists) is approximately $\geq 2k$. If a link (u, v) type is not clearly determined at a lower ($k - 1$)th layer or as a bond link at the current kth layer, it is identified as a kth-layer local bridge if and only if its $R_{u,v}^k$ common neighbor ratio exceeds a T_I^k internal threshold. In other words, a link is identified as a local bridge when its common neighbor ratio is not sufficiently high for it to be identified as a bond link ($R_{u,v}^k < T_E^k$) and when it sits in the highest non-bond link group ($R_{u,v}^k \geq T_I^k$). Note that in Fig. 3d, the common neighbor ratios for the red links exceed the 0.4471 internal threshold.

4. Global bridges. When nodes at both ends of a link do not share a friend set, endpoints can lose all connections when a bridge is removed unless alternative paths with much longer than average shortest path lengths exist. Thus, a link (u, v) is identified as a global bridge if and only if link types are not identified for all layers lower than the k_{max} layer. In Fig. 3e, since the network k_{max} layer = 1 and link (A, G) is neither a bond nor local bridge at the first layer $R_{A,G}^1 < T_I^1$, it is identified as a global bridge.

In Fig. 3 example, if the (A, G) global bridge is removed, the network is split in two. If local bridges (red lines) are removed, node E in the upper part and node G in the lower part are both split from the sub-network, and the rest of the sub-network flattens out as links connecting long-distance nodes disappear—in other words, the sub-network clustering level decreases as the network's topological structure changes. In contrast, the removal of a local bridge exerts a smaller influence on network structure—a demonstration of the replaceability difference between global and local bridges. This is also an example of how the removal of bridges from higher to lower layers reveals a node relationship hierarchy that can be used for network partitioning.

Network partitioning (sometimes referred to as community detection) is a key issue in understanding network structure [23,56], which is directly associated with link strength [5,22,57]. In this study, link type information determined by our proposed algorithm was used to develop a hierarchical recursive network community partitioning method. In the first phase the full network is partitioned into multiple highly closed communities, and in the second the same method is recursively applied to each community until it reaches a predetermined stop criterion. As shown in Algorithm 2, the hierarchical recursive network community partition method consists of four steps:

Step a. After removing all silk links from network G, the remaining isolated nodes are removed and network G' (the largest connected component in terms of the number of nodes) moves to step b.

Step b. After all global bridges are removed from network G', a determination is made as to whether the largest connected component can be partitioned into individual connected components, with each one representing a community in the highest network layer.
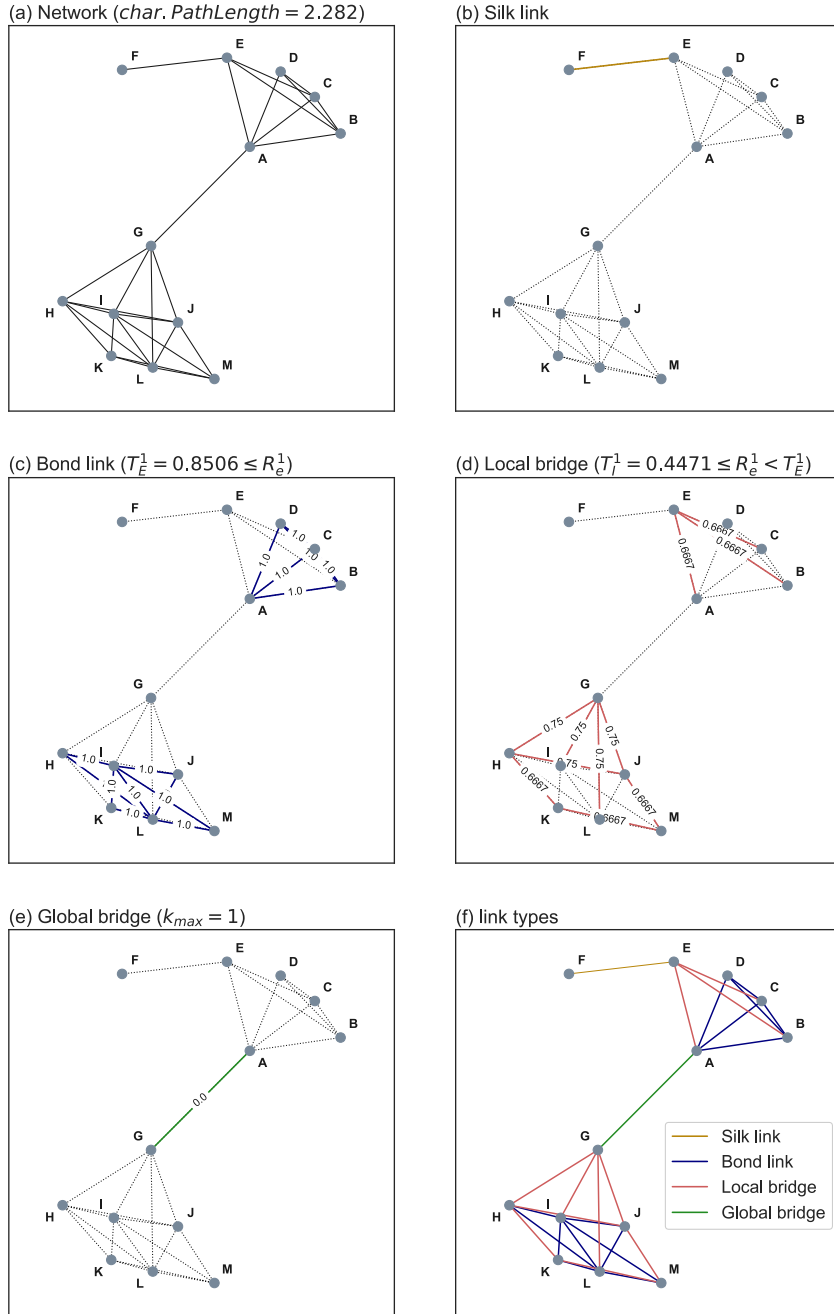
Fig. 3. Schematic diagram showing four link types: (a) the network, (b) identifying the silk links, (c) identifying the bond links, (d) identifying the first layer local bridge, (e) identifying the global bridge, and (f) the link types of all links. The average shortest path length is 2.282, thus the max-layer is 1.

Step c. After removing all kth-layer (initially $k = k_{max}$) local bridges from a connected component, a determination is made as to whether the connected component can be partitioned into individually connected sub-components, with each sub-component representing a sub-community of the kth-layer community.

Step d. When $k > 1$, let $k = k - 1$ and repeat step c. The loop ends when $k = 1$.

```
Algorithm 2 Hierarchical Network Community Partition Method
Input: network G = (V,E), where V is the node set and E the link set
Output: nested set structure NSS denoting network G hierarchical communities

Kₘₐₓ ← one-half the average shortest path length of investigated network G
c ← copy of network G
Outliers ← empty set {}
for each link (s,t) in link set E of network G do loop
    comment Step a: remove all SILK links
    if link type of link (s,t) is SILK then
       remove link (s,t) from copied network c
       if degree of node s on copied network c is 0 then
          remove node s from copied network c
          insert node s into set Outliers
       else
          remove node t from copied network c
          insert node t into set Outliers
       end if
    end if
    comment Step b: remove all GLOBAL BRIDGES
    if link type of link (s,t) is GLOBAL BRIDGE then
       remove link (s,t) from copied network c
    end if
end for
comment All independent nodes are considered as a community
NSS ← {Outliers}
for each connected component cc in copied network c do loop
    insert result returned by a recursive call component_partition(cc, Kₘₐₓ) into nested set NSS
end for
return NSS

function component_partition (network G, layer k) return nested set structure Lnss
    comment Step d: stopping conditions of recursive function
    if order of network G is equal to 1 or size of network G is equal to 0 or layer k is equal to 1 then
       return node set V of network G
    end if
    c ← copy of network G
    comment Step c: remove all kth-layer local bridges
    for each link (s,t) in link set E of network G do loop
       if link type of link (s,t) is kTH-LAYER LOCAL BRIDGE then
          remove link (s,t) from copied network c
       end if
    end for
    Lnss ← empty set {}
    for each connected component cc in copied network c do loop
       insert result returned by a recursive call component_partition(cc, (k - 1)) into nested set Lnss
    end for
return Lnss
```

3. Experimental results

3.1. First-layer common neighbor ratios

Fig. 4 presents first-layer common neighbor ratio distribution data for (a) Watts–Strogatz (WS) [32] small-world networks generated by the random rewiring of arbitrary percentages of existing links in a one-dimensional ring lattice consisting of 200 nodes (6 nearest neighbor links per node) under periodic boundary conditions, and (b) Newman–Watts (NW) [33] small-world networks generated by the addition of arbitrary percentages of additional shortcuts to a one-dimensional ring lattice consisting of 200 nodes (6 nearest neighbor links per node) under periodic boundary conditions. The data are expressed as random rewiring or shortcut probabilities. When probability p is very low – for instance, less than 0.032 ($0 \leq p \leq 0.032$) – both WS and NW small-world networks are very similar to the one-dimensional ring
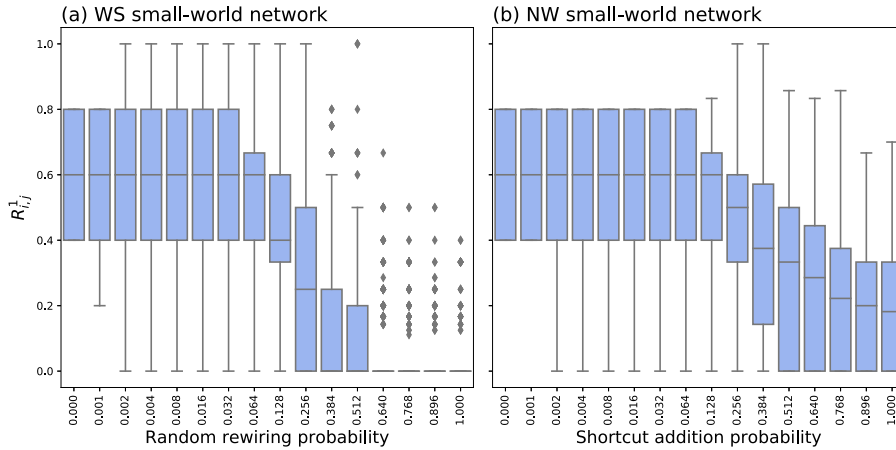
Fig. 4. Box plot of statistical distributions of first-layer common neighbor ratios: (a) Watts and Strogatz (1998) small-world networks at various random rewiring probabilities. (b) Newman and Watts (1999) small-world networks at various shortcut addition probabilities.

lattice under periodic boundary conditions. In other words, the statistical distributions of first-layer common neighbor ratios for WS small-world networks with random rewiring probabilities from 0.001 to 0.032 steadily decline within a distribution range of 0.4–0.8. When random rewiring probability $p = 0.064$, the statistical distribution of the first-layer common neighbor ratios for WS small-world networks starts to decline, becoming concentrated between 0.4 and 0.6 and decreasing as p starts increasing. When p reaches 0.64, almost all first-layer common neighbor ratios are essentially 0, with a very small number of outliers.
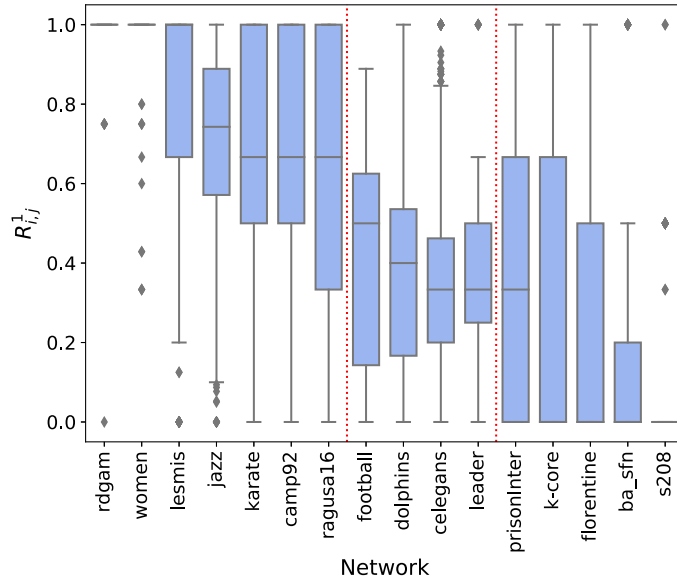
The first-layer common neighbor ratio statistical distribution for the NW small-world network started to decline when shortcut addition probability $p = 0.128$ at a distribution concentration of between 0.4 and 0.6. As p increased to 1.0, the distribution decreased and the concentration fell to between 0.0 and 0.4. Different concepts underlie the generation of WS and NW small-world networks. WS small-world networks generate shortcuts via the random rewiring of existing links, therefore the number of common neighbors is likely to decrease in response to changes in network topology. NW small-world networks generate shortcuts by adding links, resulting in the preservation of original relationships—in other words, when original common neighbors remain common neighbors, their ratios decline more slowly. When shortcut addition probability p increases, the number of links gradually increases as shortcuts are added—by definition, any shortcut essentially serves as a bridge, with nodes at both ends completely lacking common neighbors. Accordingly, first-layer common neighbor ratio distributions for NW small-world networks decrease as shortcut numbers increase.

Statistical distributions for first-layer common neighbor ratios for the 16 networks used in this study are presented as Fig. 5. As shown, these networks can be divided into three groups, separated by the two red dotted lines. The first group consists of seven networks with the largest overall common neighbor ratios. The ratio median for all links in the first three networks (rdgam, women and lesmis) was 1.0, with lesmis having fewer outlier ratios. The median for the remaining four networks was >0.6, with a higher overall centralized tendency. These results indicate that most nodes appeared in small groups with tight structures that support a larger overall common neighbor ratio distribution. For the second group (four networks), median first-layer common neighbor ratios ranged between 0.3 and 0.5, with the statistical distribution showing a tendency toward a mid-range concentration. Such a tendency suggests the presence of small groups that are tightly connected by shortcuts, resulting in low common neighbor ratios—in some cases close to 0. The third group consists of five networks with the lowest overall first-layer common neighbor ratios, with a 0.0 median for four of the five networks (prisonInter being the exception), and with higher ratios limited to very small numbers of links. Approximately half of the first-layer common neighbor ratios in prisonInter were concentrated at 0.0, approximately one-fourth at 1.0, and the remaining one-fourth between 0.0 and 1.0, pulling the entire distribution upward.
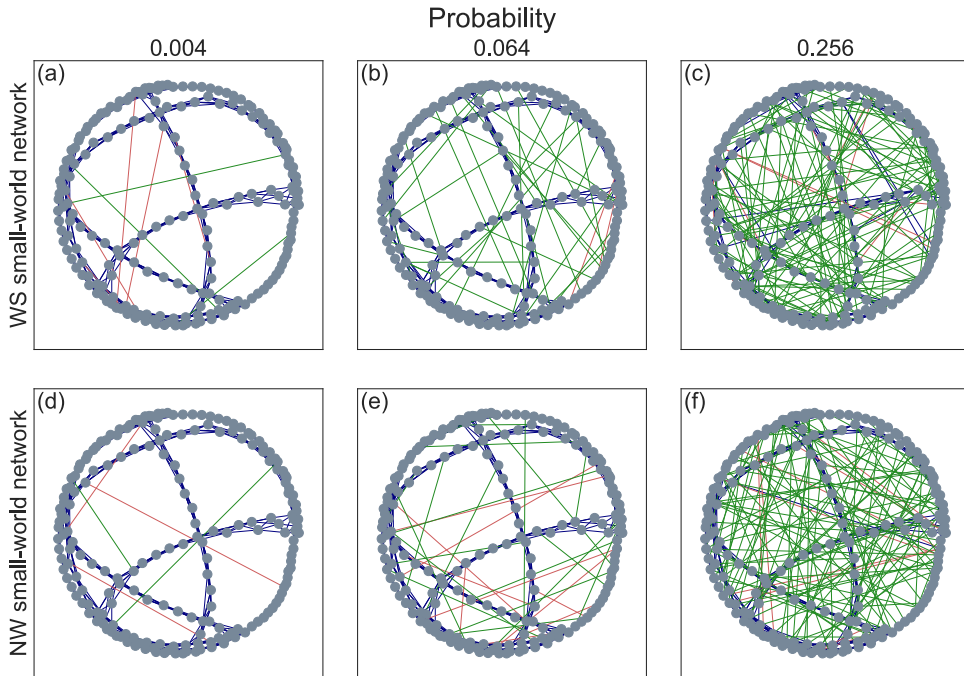
3.2. Identified network link types

Link types identified by our proposed algorithm for WS and NW small-world networks at three random rewiring and shortcut addition probabilities (0.004, 0.064 and 00.256) are presented in Fig. 6. As shown, the initial states for both network types were one-dimensional ring lattices with periodic boundary conditions, meaning that all links were bond links (no silk links). At very low probabilities (e.g., $p = 0.004$), shortcuts were easily identified as local (red line) or global bridges (green line) (Figs. 6a and 6d). As probabilities increased from 0.004 to 0.256, the number of shortcuts also increased; note the generation of more global bridges than local bridges (Figs. 6b, 6c, 6e and 6f).

Fig. 7 presents identification results for the 16 networks used in this study, arranged in the order of highest-to-lowest bond link ratio. Note the relative specificity of network topologies with higher bond link ratios, with links among small

Fig. 5. Box plot of statistical distributions of first-layer common neighbor ratios for the 16 networks used in this study.

Fig. 6. Link type identification results for Watts and Strogatz (WS) and Newman and Watts (NW) small-world networks with three random rewiring or shortcut addition probabilities: (a) WS small-world network with 0.004 random rewiring probability; (b) WS small-world network with 0.064 random rewiring probability; (c) WS small-world network with 0.256 random rewiring probability; (d) NW small-world network with 0.004 shortcut addition probability; (e) NW small-world network with 0.064 shortcut addition probability; (f) NW small-world network with 0.256 shortcut addition probability. In all networks, blue lines denote bond links, red lines local bridges, and green lines global bridges.

groups composed of bond links identified as either local (red line) or global bridges (green line). Using the rdgam, women, camp92, and karate networks as examples, 2–3 node clusters in each network are readily observable, with clusters primarily connected by green global bridges. Bond link ratios were lower in the networks toward the bottom of Fig. 6, with most links consisting of either local or global bridges. It was not possible to clearly identify clusters in these and similar networks, likely due to the small number of connections between nodes in such networks (e.g., the Barabási scale-free
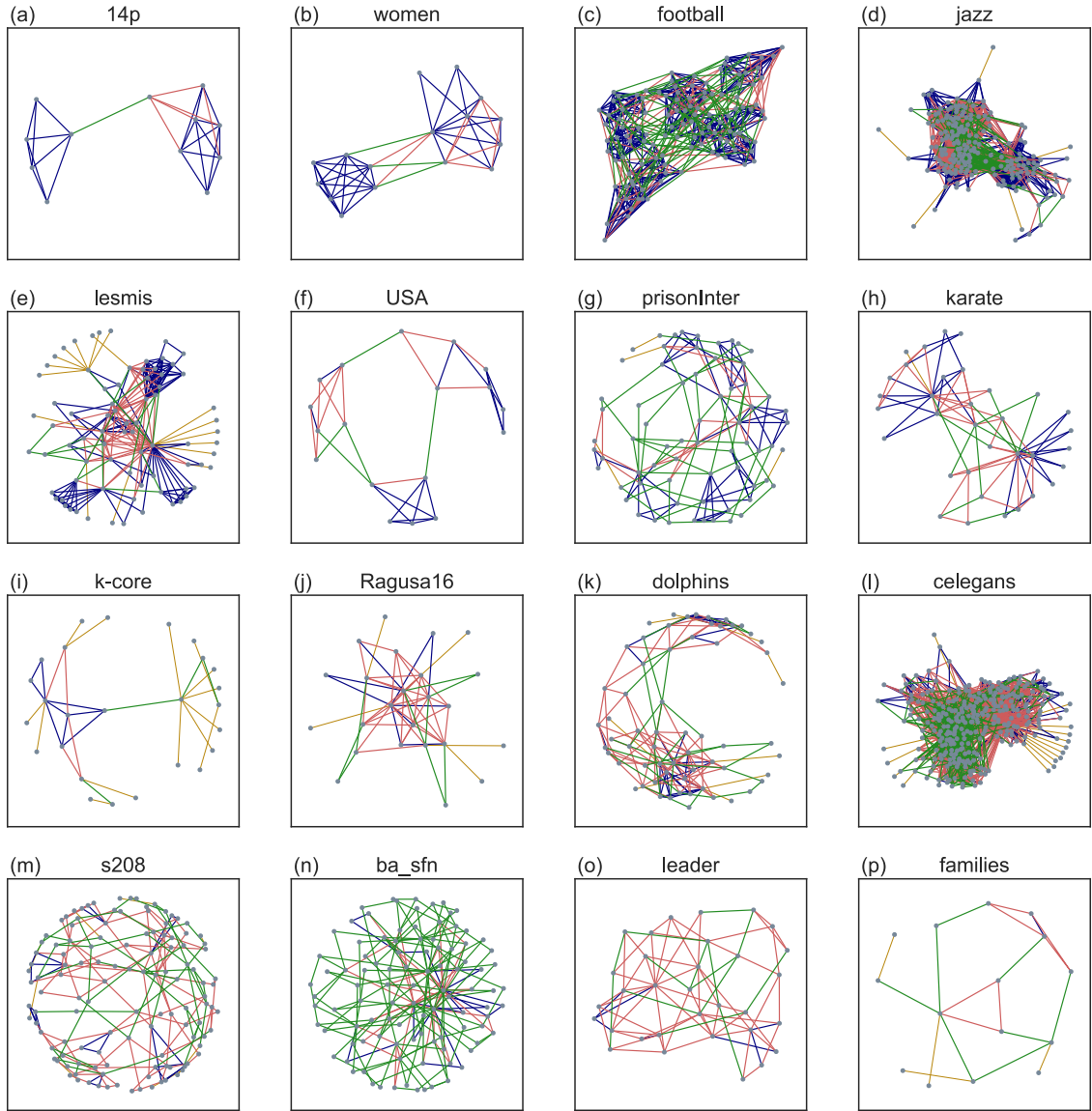
Fig. 7. Link type identification results for the 16 networks used in this study. Blue lines denote bond links, red lines local bridges, and green lines global bridges.

network [ba_sfn]), or due to the small number of nodes with tight connections, resulting in most links being identified as bridge types.

3.3. Network fingerprint comparison analysis

For comparison purposes, ratios and percentages of the four link types generated by WS small-world networks with random rewiring probabilities and NW small-world networks with shortcut addition probabilities are shown in Fig. 8. The two network types were initialized with one-dimensional ring lattices with periodic boundary conditions. Lower random rewiring and shortcut addition probabilities (i.e., between 0.0 and 0.064) indicate bond links as the primary link type. When random rewiring probability p increased from 0.128 to 1.0 in the WS small-world networks, bond link ratios started to decrease, the global bridge ratio increased rapidly from 10% to 90%, and the local bridge ratio remained within a certain range. Among the NW small-world networks, bond link ratios also decreased as the shortcut addition probability p increased from 0.128 to 1.0, but at a slower rate. At the same time, the shortcut addition probability in the NW small-world networks increased to 0.512 while the global bridge ratio increased to approximately 30% of all links, after which it remained stable within a certain range. As the shortcut addition probability p increased from 0.512 to 1.0,
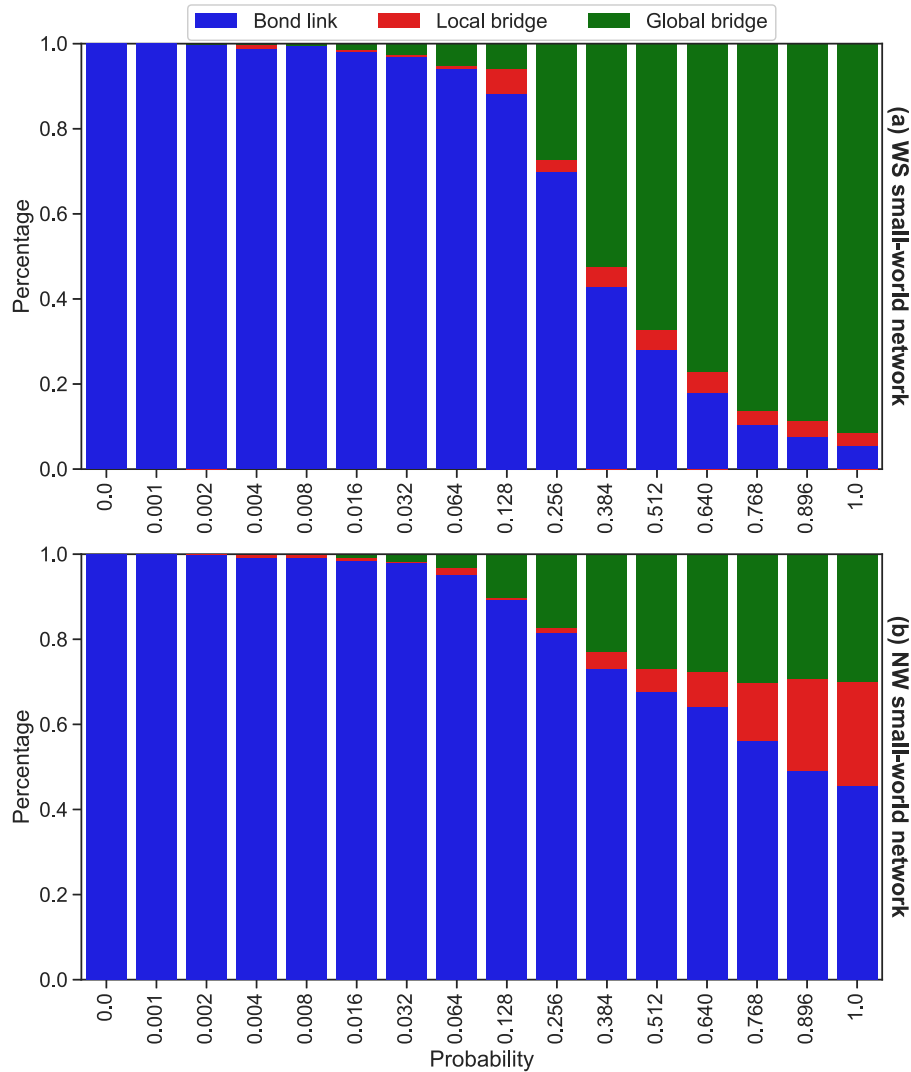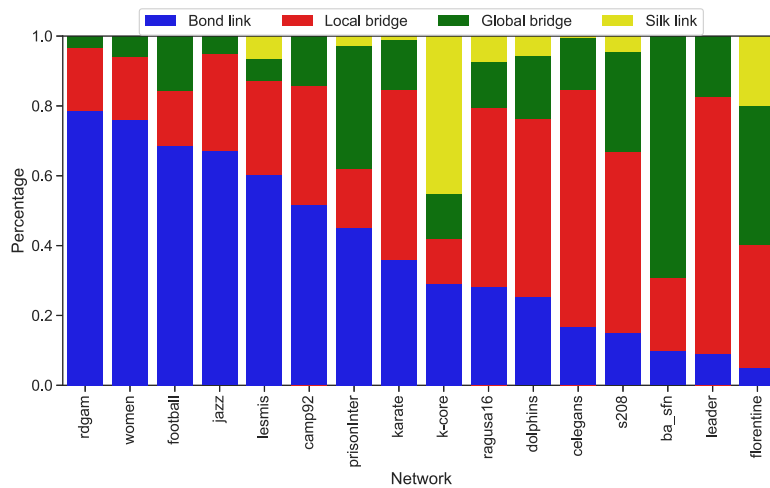
Fig. 8. Network fingerprint data for the four link types shown in Fig. 1. (a) WS small-world networks with random rewiring probabilities from 0.0 to 1.0; (b) NW small-world networks with shortcut addition probabilities from 0.0 to 1.0. Note the absence of silk links in WS small-world networks with random rewiring probabilities from 0.0 to 1.0 and NW small-world networks with shortcut addition probabilities from 0.0 to 1.0.

the local bridge ratio gradually increased to approximately 30% of all links at the same probability that the bond link ratio decreased.

Our fingerprint analysis results successfully captured similarities and differences between the WS and NW small-world networks. Specifically, they indicate that in the WS small-world networks, normal and tighter relationships between links were affected as random rewiring probabilities increased, and bond link ratios had the potential to rapidly decrease when random rewiring probabilities were high. However, in NW small-world networks such close relationships were not directly damaged by increases in shortcut addition probability; note that the bond link ratio remained within 45% regardless of any increase in that probability. In the NW small-world networks, when the relationship between stable bond links did not experience damage, increases were observed in both overall network density and shortcut addition probability—in other words, the number of links grew. Due to this increase in link number, additional shortcuts likely resulted in new bond link relationships at higher levels, with a significant number of shortcuts having sufficiently high common neighbor ratios so that an increase in average clustering value was extended by two or more path steps, with shortcut links consequently becoming local bridges.

Fig. 9 presents our network fingerprint analysis results for the 16 networks used in this study, arranged from highest-to-lowest bond link ratio. Note the clearly observable differences in distributions between these networks and the WS and NW small-world networks: most of the 16 networks primarily consist of bond links or local bridges, with their sums exceeding 80% of all links in 11 of the 16 networks, 60% in two others, and less than 50% in three (i.e., k-core, ba-sfn and

Fig. 9. Network fingerprint data for the four link types shown in Fig. 1 in the 16 networks used in this study.
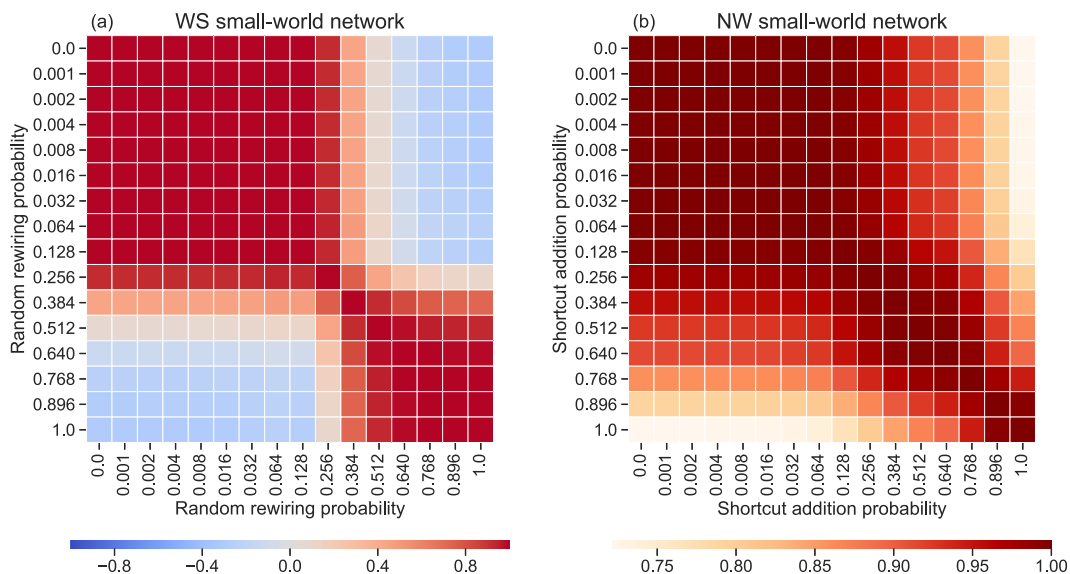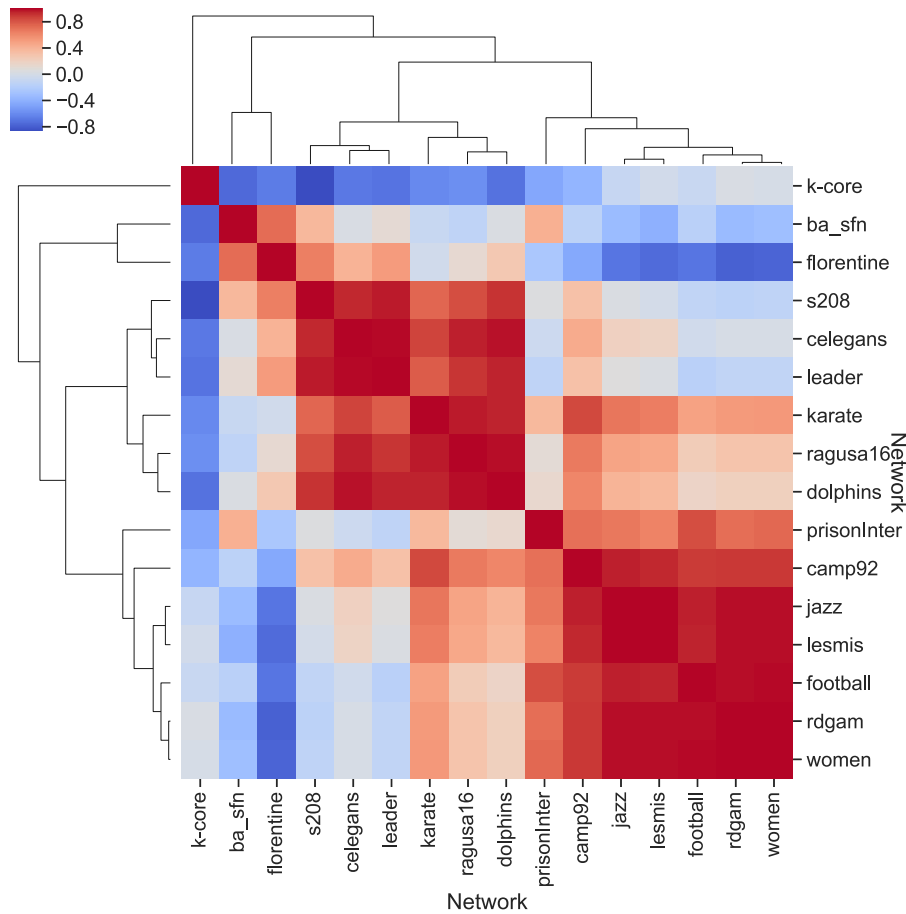

Fig. 10. Correlation coefficient matrix data at various link type percentages for (a) WS small-world networks with random rewiring probabilities from 0.0 to 1.0 and (b) NW small-world networks with shortcut addition probabilities from 0.0 to 1.0.

florentine). Almost one-half of the k-core network consists of silk links, making it impossible to show group structures (Fig. 7i). The ba-sfn network had a high global bridge ratio (approximately 70%) and greater resemblance with the WS small-world network structure compared to the k-core and florentine networks (the main difference being more local bridges in the ba-sfn network). The florentine network had the lowest bond link ratio and the second highest silk link ratio, and its local bridge and global bridge ratios comprised one-half of the remaining ratios, indicating that it may have been completely free of small groups, with most nodes connected by bridge-type links.

Our fingerprint analysis data support the idea of using network topological similarities and differences in fingerprint structure with correlation matrices. Matrix graphs for the two types of small-world networks according to random rewiring and shortcut addition probabilities from 0.0 to 1.0 are shown in Fig. 10. The two network types expressed different fingerprint change trends as probabilities increased. The WS small-world network produced two clearly distinguishable sub-matrices, one with fingerprints ranging from 0.0 to 0.256 and the other from 0.384 to 1.0 (−0.4 correlation coefficient, indicating an increase followed by a decrease, with the turning point located between 0.256 and 0.384). The NW small-world network had a minimum overall correlation coefficient of 0.7, indicating that all of the NW small-world networks we looked at were similar.

Compared with the results shown in Fig. 8, the early-stage WS small-world networks primarily consisted of blue bond links, but subsequent network changes were primarily formed by green global bridges at a random rewiring probability

Fig. 11. Correlation coefficient matrix data at various link type percentages for the 16 networks used in this study.

of 0.384 or higher. Early-stage NW small-world networks also primarily consisted of bond links, but higher numbers of local or global bridges emerged following the addition of shortcuts; bond links were still predominant, and few changes were observed in the global bridge ratio.

Results from our fingerprint correlation matrix analysis of the 16 networks used in this research are consistent with those shown in Figs. 4 and 8. As indicated in Fig. 11, the two main group network types were those primarily consisting of local bridges (6 networks, from s208 to dolphins) or bond links (7 networks, from prisonInter to women). For the most part, these two groups exhibited uncorrelated structures; two important exceptions were karate and camp92, each of which shared certain similarities with networks in their counterpart groups.

Our proposed fingerprint analysis framework consists of ratio distributions for the four link types plus network similarity comparisons using the correlation coefficient matrix. We found that the four link types were capable of capturing network topologies up to a certain point, after which similarities in network topologies could be further analyzed in terms of fingerprints involving node number, link number, the centrality distribution of node branching, and other network properties. It is our assertion that all network topologies are classifiable, and that similarities in network topologies can be identified via fingerprint comparisons.

3.4. Network partition results

We categorized the 16 networks according to partition results produced by our proposed algorithm (Fig. 12, Table 2). Note that Fig. 12a has two group nodes (green and blue) and one independent gray node. Links between green group nodes are all of the bond type, with four local bridges connecting the independent gray node to blue group nodes that are not connected to green group nodes. Fig. 12b shows two groups of nodes with global or local bridges between them, and Fig. 12c shows two major group nodes (blue and green) and two small group nodes lacking sufficiently close links; in most cases these nodes are connected by local bridges. The network displayed in Fig. 12d consists of two major groups (blue and green) of nodes connected by global or local bridges, with some independent gray nodes in the middle.
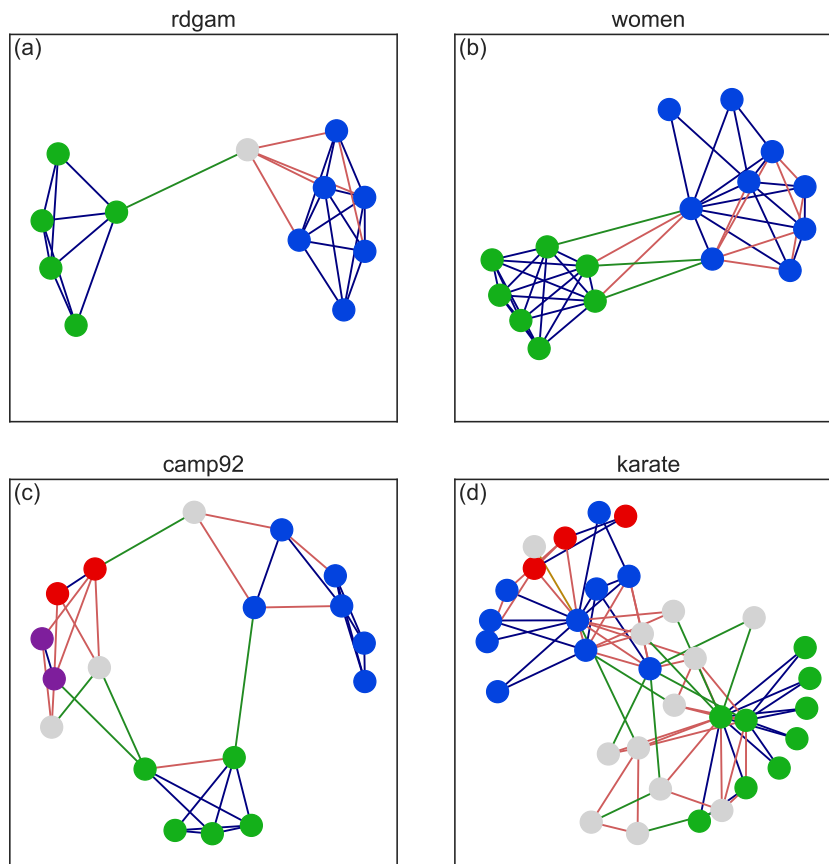
Fig. 12. Hierarchical network community partition results for four networks: (a) rdgam, (b) women, (c) camp92 and (d) karate. Green lines, global bridges; red lines, local bridges; blue lines, bond links; yellow lines, silk links.

Table 2
Hierarchical network community partition results for the 16 networks listed in Table 1.

	Network code	Group number	Independent node[a] number	Total number of nodes in all groups	Average group density	Weighted average of all links within groups[b]	Weighted average of all links between groups[c]
1	rdgam	3	1	11	0.92 (0.02)	0.99 (0.05)	0.60 (0.30)
2	women	2	0	16	0.83 (0.17)	0.96 (0.10)	0.37 (0.05)
3	football	5	0	115	0.59 (0.29)	0.50 (0.21)	0.05 (0.07)
4	jazz	10	7	191	0.42 (0.41)	0.72 (0.20)	0.64 (0.29)
5	lesmis	16	8	69	0.70 (0.31)	0.89 (0.25)	0.56 (0.33)
6	camp92	7	3	15	0.89 (0.14)	0.85 (0.23)	0.31 (0.23)
7	prisonInter	29	22	45	0.60 (0.34)	0.72 (0.26)	0.07 (0.13)
8	karate	15	12	22	0.61 (0.27)	0.93 (0.15)	0.39 (0.28)
9	k-core	11	9	17	0.32 (0.28)	0.67 (0.35)	0.07 (0.13)
10	ragusa16	18	15	9	1.50 (0.71)	0.69 (0.30)	0.55 (0.35)
11	dolphins	36	30	32	0.67 (0.32)	0.61 (0.21)	0.30 (0.24)
12	celegans	116	96	201	0.68 (0.31)	0.47 (0.19)	0.27 (0.18)
13	s208	96	87	35	0.85 (0.31)	0.52 (0.14)	0.00 (0.00)
14	ba_sfn	82	80	20	0.60 (0.40)	0.71 (0.37)	0.06 (0.14)
15	leader	25	21	11	1.00 (0.00)	0.83 (0.22)	0.31 (0.20)
16	florentine	11	9	6	0.50 (0.50)	1.00 (0.00)	0.18 (0.24)

[a]Since our proposed community partition does not require the inclusion of individual nodes into specific groups, some independent nodes were not placed in any community, and therefore remain outside of detected groups.
[b]Weighted average of all links within groups: average first-layer common neighbor ratios (standard deviations in parentheses).
[c]Weighted average of all links between groups: average first-layer common neighbor ratios after breaking up the main group (standard deviations in parentheses).

4. Conclusion

Even though local and global bridges play important roles in ensuring network connectivity, the notion of local or global bridges in networks has never been systematically investigated. In this paper we addressed the importance of links and the roles they play in network topologies, and proposed a hierarchical edge type analysis (HETA) algorithm for determining link types at all layers in a given network based on the common neighbor concept and statistical factors. The primary function of the proposed algorithm is to identify bond links, kth-layer local bridges, global bridges, and silk links. The basic common neighbor concept refers to the degree to which nodes at both ends of a link know each other's neighbors. In the event of neighbor overlap, or if one node knows all of the neighbors of other nodes, then the link is said to be in the middle of a close group. If the two nodes have no common neighbors, the link is said to be located between two distinct groups. The first scenario indicates the presence of one or more bond links within a network's topological structure, and the second the presence of a bridge, and our results indicate that the proposed algorithm is capable of identifying both. In acknowledgment of quantitative and statistical differences, we also addressed changes in link strength during the transition from bond links to global bridges via kth-layer local bridges. After calculating common neighbor ratios for all links at all layers of a given network, we applied an ensemble of randomized networks corresponding to a given network to distinguish among link types. Our findings indicate that the common neighbor ratios of bond links across networks differed according to the number of nodes, the number of links, and the node degree distribution: in networks with more links, the common neighbor ratio for each link was higher, even in cases of random connections. According to these findings, a fixed ratio is not suitable for determining the presence of a bond link. Instead, when the common neighbor ratio exceeds an external threshold, then 1,000 corresponding randomized networks for each target network should be used to calculate the external thresholds of individual layers.

Using two types of small-world networks to validate our proposed algorithm, we found that the number of shortcuts gradually increased as the probability of random rewiring or shortcut addition increased, thus confirming that the algorithm is capable of detecting such shortcuts. Further, results from our comparison of the two small-world network types with the same probability parameter indicate that the networks generated by the random rewiring probability experienced greater damage to their topological structure compared to those generated by the shortcut addition probability. This difference was also observable in our common neighbor ratio results, as well as in the ratio distributions for each type produced by a network fingerprint analysis. After using 16 well-known networks found in the literature to demonstrate our proposed algorithm's ability to capture local and global bridges, the topological structures of most networks were clearly observable, including bond links and local/global bridges at each network layer. Complex structures in networks lacking obvious bond links or local/global bridges were also observed.

After using our proposed algorithm to identify the micro- and macro-level impacts of a link on a network, it is possible to establish optimum network strategies involving the four link types for application to real-life scenarios such as controlling the spread of rumors or enduring attacks on P2P-related service infrastructures. For example, after determining bond links and local/global bridges in an Internet topology, global bridges can be strengthened to ensure the long-distance delivery of information, thus improving overall reliability. In situations involving communicable disease networks, if different epidemic intervention policies can be employed by public health agencies for specifically identified link types, the spread of an infectious disease can be controlled in a more cost-effective manner. Our proposed algorithm and experimental results can help network researchers in studies of complex real-world and theoretical network architectures, perhaps assisting in the distributed design of robust networks meant to resist link attacks. It is still necessary to generalize hierarchical local/global bridge definitions when addressing other network configurations such as bipartite networks. Our plans are to perform empirical analyses with higher numbers of large-scale networks.

Acknowledgment

References

[1] M.G. Everett, S.P. Borgatti, The centrality of groups and classes, J. Math. Sociol. 23 (1999) 181–201, http://dx.doi.org/10.1080/0022250X.1999.9990219.

[2] M.S. Granovetter, The strength of weak ties, Am. J. Sociol. 78 (1973) 1360–1380, http://dx.doi.org/10.1086/225469.

[3] P. Csermely, Weak Links: Stabilizers of Complex Systems from Proteins to Social Networks, first ed., Springer, Berlin; New York, 2006.

[4] K. McCann, A. Hastings, G.R. Huxel, Weak trophic interactions and the balance of nature, Nature 395 (1998) 794–798, http://dx.doi.org/10.1038/27427.

[5] H. Lee, N. Kwak, S.W. Campbell, Hearing the other side revisited: the joint workings of cross-cutting discussion and strong tie homogeneity in facilitating deliberative and participatory democracy, Commun. Res. 42 (2015) 569–596, http://dx.doi.org/10.1177/0093650213483824.

[6] O. Torro, J.P. Gupta, H. Kärkkäinen, H. Pirkkalainen, R. Vatrapu, R.R. Mukkamala, A. Hussain, Integrating micro-level interactions with social network analysis in tie strength research: The edge-centered approach, in: Proc. 21st Int. Acad. Mindtrek Conf. - Acad. 17, ACM Press, Tampere, Finland, 2017, pp. 203–209, http://dx.doi.org/10.1145/3131085.3131095.

[7] M.T. Hansen, The search-transfer problem: the role of weak ties in sharing knowledge across organization subunits, Adm. Sci. Q. 44 (1999) 82–111, http://dx.doi.org/10.2307/2667032.

[8] R.D. Putnam, Bowling alone: The collapse and revival of American community, 1. touchstone ed., Simon & Schuster, New York, NY, 2001.

[9] M. Burke, R.E. Kraut, The relationship between Facebook use and well-being depends on communication type and tie strength: Facebook and well-being, J. Comput. Mediat. Commun. 21 (2016) 265–281, http://dx.doi.org/10.1111/jcc4.12162.

[10] L.K. Gee, J. Jones, M. Burke, Social networks and labor markets: How strong ties relate to job finding on Facebook's social network, J. Labor Econ. 35 (2017) 485–518, http://dx.doi.org/10.1086/686225.

[11] B.O. Holzbauer, B.K. Szymanski, T. Nguyen, A. Pentland, Social ties as predictors of economic development, in: A. Wierzbicki, U. Brandes, F. Schweitzer, D. Pedreschi (Eds.), Adv. Netw. Sci, Springer International Publishing, Cham, 2016, pp. 178–185, http://dx.doi.org/10.1007/978-3-319-28361-6_15.

[12] P. Luarn, Y.-P. Chiu, Key variables to predict tie strength on social network sites, Internet Res. 25 (2015) 218–238, http://dx.doi.org/10.1108/IntR-11-2013-0231.

[13] D. Wegge, H. Vandebosch, S. Eggermont, M. Walrave, The strong the weak and the unbalanced: The link between tie strength and cyberaggression on a social network site, Soc. Sci. Comput. Rev. 33 (2015) 315–342, http://dx.doi.org/10.1177/0894439314546729.

[14] A. Clauset, C. Moore, M.E.J. Newman, Hierarchical structure and the prediction of missing links in networks, Nature 453 (2008) 98–101, http://dx.doi.org/10.1038/nature06830.

[15] Y.-H. Fu, C.-Y. Huang, C.-T. Sun, A community detection algorithm using network topologies and rule-based hierarchical arc-merging strategies, PLOS ONE 12 (2017) e0187603, http://dx.doi.org/10.1371/journal.pone.0187603.

[16] S. Goyal, Connections: An introduction to the economics of networks, 2012, http://grail.eblib.com.au/patron/FullRecord.aspx?p=483551. (Accessed 1 November 2018).

[17] A. Barrat, M. Barthelemy, R. Pastor-Satorras, A. Vespignani, The architecture of complex weighted networks, Proc. Natl. Acad. Sci. 101 (2004) 3747–3752, http://dx.doi.org/10.1073/pnas.0400087101.

[18] J.-P. Onnela, J. Saramaki, J. Hyvonen, G. Szabo, D. Lazer, K. Kaski, J. Kertesz, A.-L. Barabasi, Structure and tie strengths in mobile communication networks, Proc. Natl. Acad. Sci. 104 (2007) 7332–7336, http://dx.doi.org/10.1073/pnas.0610245104.

[19] N.V. Papakyriazis, M.A. Boudourides, Electronic weak ties in network organisations, Goettingen, Germany, 2001. http://citeseerx.ist.psu.edu/viewdoc/summary?doi=10.1.1.25.3459.

[20] M.K. Sohrabi, S. Akbari, A comprehensive study on the effects of using data mining techniques to predict tie strength, Comput. Human Behav. 60 (2016) 534–541, http://dx.doi.org/10.1016/j.chb.2016.02.092.

[21] A.-K. Wu, L. Tian, Y.-Y. Liu, Bridges in complex networks, Phys. Rev. E. 97 (2018) http://dx.doi.org/10.1103/PhysRevE.97.012307.

[22] M. Girvan, M.E.J. Newman, Community structure in social and biological networks, Proc. Natl. Acad. Sci. 99 (2002) 7821–7826, http://dx.doi.org/10.1073/pnas.122653799.

[23] R. Shang, W. Zhang, L. Jiao, R. Stolkin, Y. Xue, A community integration strategy based on an improved modularity density increment for large-scale networks, Physica A 469 (2017) 471–485, http://dx.doi.org/10.1016/j.physa.2016.11.066.

[24] B. Min, F. Liljeros, H.A. Makse, Finding influential spreaders from human activity beyond network location, PLOS ONE 10 (2015) e0136831, http://dx.doi.org/10.1371/journal.pone.0136831.

[25] P. Wang, B. Xu, Y. Wu, X. Zhou, Link prediction in social networks: The state-of-the-art, Sci. China Inf. Sci. 58 (2015) 1–38, http://dx.doi.org/10.1007/s11432-014-5237-y.

[26] J.E. Perry-Smith, Social network ties beyond nonredundancy: An experimental investigation of the effect of knowledge content and tie strength on creativity., J. Appl. Psychol. 99 (2014) 831–846, http://dx.doi.org/10.1037/a0036385.

[27] P. Jensen, M. Morini, M. Karsai, T. Venturini, A. Vespignani, M. Jacomy, J.-P. Cointet, P. Mercklé, E. Fleury, Detecting global bridges in networks, J. Complex Netw. 4 (2016) 319–329, http://dx.doi.org/10.1093/comnet/cnv022.

[28] S. Aral, The future of weak ties, Am. J. Sociol. 121 (2016) 1931–1939, http://dx.doi.org/10.1086/686293.

[29] J. Bruggeman, The strength of varying tie strength, 2012, ArXiv12125969 Phys. http://arxiv.org/abs/1212.5969. (Accessed 1 November 2018).

[30] C. Ma, T. Zhou, H.-F. Zhang, Playing the role of weak clique property in link prediction: A friend recommendation model, Sci. Rep. 6 (2016) http://dx.doi.org/10.1038/srep30098.

[31] B. Bollobás, Modern Graph Theory, Springer, New York, 1998.

[32] D.J. Watts, S.H. Strogatz, Collective dynamics of 'small-world' networks, Nature 393 (1998) 440–442, http://dx.doi.org/10.1038/30918.

[33] M.E.J. Newman, D.J. Watts, Renormalization group analysis of the small-world network model, Phys. Lett. A 263 (1999) 341–346, http://dx.doi.org/10.1016/S0375-9601(99)00757-4.

[34] F.J. Roethlisberger, W.J. Dickson, H.A. Wright, Management and the Worker: An Account of a Research Program Conducted by the Western Electric Company, Hawthorne Works, Chicago, 16 printing, Harvard Univ. Press, Cambridge, Mass, 1939.

[35] A. Davis, B.B. Gardner, M.R. Gardner, Deep South: A Social Anthropological Study of Caste and Class, Pbk. ed, University of South Carolina Press, Columbia, S.C, 2009.

[36] M.E.J. Newman, Modularity and community structure in networks, Proc. Natl. Acad. Sci. 103 (2006) 8577–8582, http://dx.doi.org/10.1073/pnas.0601602103.

[37] P.M. Gleiser, L. Danon, Community structure in jazz, Adv. Complex Syst. 06 (2003) 565–573, http://dx.doi.org/10.1142/S0219525903001067.

[38] D.E. Knuth, The Stanford GraphBase: A Platform for Combinatorial Computing, ACM Press, Addison-Wesley, New York, N.Y.: Reading, Mass, 1993.

[39] S.P. Borgatti, M.G. Everett, L.C. Freeman, UCINET 5 for Windows, Analytic Technologies, Inc. and University of Greenwich, Natick, 1999.

[40] R. Milo, S. Shen-Orr, S. Itzkovitz, N. Kashtan, D. Chklovskii, U. Alon, Network motifs: Simple building blocks of complex networks, Science 298 (2002) 824–827, http://dx.doi.org/10.1126/science.298.5594.824.

[41] D. MacRae, Direct factor analysis of sociometric data, Sociometry 23 (1960) 360, http://dx.doi.org/10.2307/2785690.

[42] W.W. Zachary, An information flow model for conflict and fission in small groups, J. Anthropol. Res. 33 (1977) 452–473, http://dx.doi.org/10.1086/jar.33.4.3629752.

[43] L.D. Zeleny, Adaptation of research findings in social leadership to college classroom procedures, Sociometry 13 (1950) 314, http://dx.doi.org/10.2307/2785274.

[44] V. Batagelj, in: A. Ferligoj, A. Kramberger (Eds.), Ragusan Families Marriage Networks, in: Dev. Data Anal., FDV, Ljubljana, 1996, pp. 217–228.

[45] D. Lusseau, K. Schneider, O.J. Boisseau, P. Haase, E. Slooten, S.M. Dawson, The bottlenose dolphin community of doubtful sound features a large proportion of long-lasting associations, Behav. Ecol. Sociobiol. 54 (2003) 396– 405, http://dx.doi.org/10.1007/s00265-003-0651-y.

[46] R.L. Breiger, P.E. Pattison, Cumulated social roles: The duality of persons and their algebras, Soc. Netw. 8 (1986) 215–256, http://dx.doi.org/10.1016/0378-8733(86)90006-7.

[47] J.G. White, E. Southgate, J.N. Thomson, S. Brenner, The structure of the nervous system of the nematode caenorhabditis elegans, Philos. Trans. R. Soc. Lond. B. Biol. Sci. 314 (1986) 1–340.

[48] R. Albert, A.-L. Barabási, Statistical mechanics of complex networks, Rev. Modern Phys. 74 (2002) 47–97, http://dx.doi.org/10.1103/RevModPhys.74.47.

[49] R.F. i Cancho, C. Janssen, R.V. Solé, Topology of technology graphs: small world patterns in electronic circuits, Phys. Rev. E. 64 (2001).

[50] A.-L. Barabási, R. Albert, Emergence of scaling in random networks, Science 286 (1999) 509–512, http://dx.doi.org/10.1126/science.286.5439.509.

[51] J. Bae, S. Kim, Identifying and ranking influential spreaders in complex networks by neighborhood coreness, Phys. Stat. Mech. Appl. 395 (2014) 549–559, http://dx.doi.org/10.1016/j.physa.2013.10.047.

[52] M.E.J. Newman, S.H. Strogatz, D.J. Watts, Random graphs with arbitrary degree distributions and their applications, Phys. Rev. E 64 (2001) http://dx.doi.org/10.1103/PhysRevE.64.026118.

[53] C.-Y. Huang, C.-Y. Cheng, C.-T. Sun, Bridge and brick network motifs: identifying significant building blocks from complex biological systems, Artif. Intell. Med. 41 (2007) 117–127, http://dx.doi.org/10.1016/j.artmed.2007.07.006.

[54] R. Milo, N. Kashtan, S. Itzkovitz, M.E.J. Newman, U. Alon, On the uniform generation of random graphs with prescribed degree sequences, 2003, ArXivcond-Mat0312028. http://arxiv.org/abs/cond-mat/0312028. (Accessed 1 November 2018).

[55] R. Milo, S. Itzkovitz, N. Kashtan, R. Levitt, S. Shen-Orr, I. Ayzenshtat, M. Sheffer, U. Alon, Superfamilies of evolved and designed networks, Science 303 (2004) 1538–1542, http://dx.doi.org/10.1126/science.1089167.

[56] R. Shang, W. Zhang, L. Jiao, Circularly searching core nodes based label propagation algorithm for community detection, Int. J. Pattern Recognit. Artif. Intell. 30 (2016) 1659024, http://dx.doi.org/10.1142/S0218001416590242.

[57] P. De Meo, E. Ferrara, G. Fiumara, A. Provetti, On Facebook, most ties are weak, Commun. ACM. 57 (2014) 78–84, http://dx.doi.org/10.1145/2629438.